Journal of Electroanalytical Chemistry, 361 (1993) 251–256

JEC 02838

Short communication

Investigation of microelectrodes
IX: Study of the edge effects at a microdisk electrode

Ju Huangxian, Chen Hongyuan * and Gao Hong

Department of Chemistry, Nanjing University, Nanjing 210008 (China)

(Received 27 January 1992; in revised form 16 March 1993)

1. Introduction

The behaviour of microdisk electrodes has attracted much notice, owing to their strong edge effect [1,2]. The diffusion regions at these electrodes have been studied theoretically [2–9]. In order to describe the mass transport rate at a microdisk electrode, some authors [1,8,9] have compared the current density and the mass transport rate at the microdisk electrode with those at a rotating disk electrode, but the results were quite different, even for electrodes of identical radius. However, these data have often been cited in various situations to characterize the mass transfer efficiency of the microdisk electrode, producing a confusion of data. Thus, it is necessary to study further the basic problem and to establish a reasonable kinetic model. Our work describes the relations of the current density and the mass transport rate between these two types of electrode. Furthermore, the edge effect of the microdisk electrode can be illustrated using these relations.

At a low scan rate, the cyclic voltammogram of a microdisk electrode is a "sigmoid" curve, owing to the effect of radial diffusion, i.e. the forward and backward sweep curves overlap each other, and only one kind of electrode reaction occurs. However, the two sweeps of the cyclic voltammogram separate gradually with increasing scan rate, and appear as two neighbouring curves, denoted the "retention cycle". Because the inverse reaction occurs during the backward sweep, the total current is composed of the currents of the positive reaction I_O and the inverse reaction I_R. Galus et al. [3] determined a relation for the two currents:

$$\frac{I_O}{I_R} = 1 + Q\frac{(DRT)^{1/2}}{(nF\nu)^{1/2}r} \qquad (Q = 0.92) \qquad (1)$$

* To whom correspondence should be addressed.

However, they did not consider it possible to determine I_R at such an electrode. Zoski et al. [10] suggested that the discrepancy between the currents of the forward and backward sweeps depends on the magnitude of the parameter $(nF\nu d^2/RTD)^{1/2}$. In this work, a method to determine I_R is presented. A formula for calculating the concentration of the product in the reaction area on the electrode surface is proposed. The concept of the retention effect is suggested, and the retention effect is described quantitatively by the coefficient of retention.

2. Theory

For a reversible reaction $R \rightleftharpoons O + ne^-$, when $D_R = D_O = D$, the steady-state limiting current of single sweep voltammetry for a low scan rate at a microdisk electrode is [11]

$$I_{d(mde)} = 4nFc_R^* Dr \qquad (2)$$

where all the symbols have their usual meaning. The steady-state mass transport coefficient at the microdisk electrode is

$$(m_{ss})_1 = I_{d(mde)}/nFAc_R^* = 4D/\pi r \qquad (3)$$

and the mass transport coefficient at a rotating disk electrode is

$$(m_{ss})_2 = I_{a(rde)}/nFAc_R^* = 0.62D^{2/3}\omega^{1/2}\nu^{-1/6} \qquad (4)$$

Thus, the relation between the radius of a microdisk electrode and the speed of rotation of a rotating disk electrode under the condition of equal mass transport coefficient can be expressed as

$$\omega = 4.22D^{2/3}\nu^{1/3}/r^2 \qquad (5)$$

If the following parameters are designated the same as in the literature [9], i.e. $\nu = 5 \times 10^{-3}$ cm^2 s^{-1} and $D = 5 \times 10^{-6}$ cm^2 s^{-1}, then when $r = 5$ μm, 4 μm and

0022-0728/93/$6.00

0.5 μm, the corresponding speeds of rotation are 8064, 12600 and 806400 rev min^{-1} (1 rev $min^{-1} = 2\pi$ rad min^{-1}) respectively for equal mass transport coefficients, but the values given in the literature are 10000 [9], 30000 [1], and 1224000 [8] rev min^{-1} respectively. There is thus a disagreement.

The above result means that the steady-state mass transport at a microdisk electrode is much faster than that at a regular size disk electrode. This is due to the spherical diffusion taking place at such an electrode. It increases the current density greatly. The ratio of the current density at a microdisk electrode to that at a large disk electrode is

$$j_{ss}/j = 4D^{1/2}t^{1/2}/\pi^{1/2}r \quad (6)$$

and the ratio of the current density at a microdisk electrode to that at a rotating disk electrode is

$$j_{ss}/j_{rde} = 2.05D^{1/3}\nu^{1/6}/\omega^{1/2}r \quad (7)$$

The steady-state contributions to the current at a microdisk electrode have been referred to colloquially as the edge effect (or at a spherical electrode, as the spherical effect [1]. They not only increase the current density, but also make the cyclic voltammogram similar to a d.c. polarogram. In the ideal case, the single electrode reaction (reduction or oxidation), which depends on the initial state of electroactive species in solution, occurs instead of the redox couple reaction. Because the diffusion of the product is so fast that the electrode surface can always remain in the initial state, the two branches of the cyclic voltammogram overlap to form a typical "sigmoid" curve. With increasing scan rate, the rate of the electrode reaction becomes greater than the rate of mass transport, and part of the product remains in the region of the electrode surface. Therefore, the two kinds of electrode reaction occur, and the sigmoid-type overlapping cyclic voltammogram begins to split up into two adjacent curves. In other words, the so-called "cycle of retention" is formed, which reveals the deviation of the actual voltammogram from the ideal sigmoid curve. The area of the cycle of retention depends on the scan rate.

At a low scan rate, the total currents I in both the forward and backward sweep are the sum of the Faradaic current I_f and the capacitance current I_z, i.e. $I = I_f + I_z$; the current in the first forward sweep is

$$I_{a(E)} = I_{O(E)} + (I_{z(E)})_a \quad (8)$$

and the current in the backward sweep contains three parts:

$$I_{c(E)} = (I_{O(E)})' + I_{R(E)} + (I_{z(E)})_c \quad (9)$$

where I_O is the oxidation current and I_R is the reduction current. In the case of steady-state mass transport, $I_{O(E)} = (I_{O(E)})'$. When the scan rate is identical, $(I_{z(E)})_a = -(I_{z(E)})_c = I_{z(E)}$ can be obtained from the cyclic voltammogram of the blank solution. Thus $I_{R(E)}$, the inverse reaction current for $R \rightleftharpoons O + ne^-$, can be expressed as

$$I_{R(E)} = I_{c(E)} - I_{a(E)} - 2I_{z(E)} \quad (10)$$

The inverse reaction current can be found. At the limiting current, c_R^s (the concentration of the reactant in the area of the electrode surface) is much smaller than the bulk concentration, and c_O (the concentration of the product in the area of the electrode surface) is c_R^*. During the backward sweep, the product diffuses away from the electrode surface. When the scan rate increases, a part of the product remains in the area of the electrode surface since there is not enough time for it to leave; its concentration is c_O^s. That is the so-called "retention effect". When the potential is sufficiently negative, the product with concentration c_O^s at the electrode surface can be reduced. The reduction current is

$$I_{R(E)} = 4nFDc_O^s r \quad (11)$$

Thus, c_O^s can be obtained from eqns. (2) and (11), i.e.

$$c_O^s = I_{R(E)}c_R^*/I_{d(mde)} \quad (12)$$

In order to describe the extent of retention, the ratio of the concentration of product remaining in the reaction area c_O^s to the initial concentration of the product formed on the electrode surface c_O is defined as the coefficient of retention K_s:

$$K_s = c_O^s/c_O = I_{R(E)}/I_{d(mde)} \quad (13)$$

It is obvious that the retention effect leads to deviation of the cyclic voltammogram from the ideal steady-state curve, and two neighbouring sigmoidal curves are obtained. Their shapes and the extent of separation depend on the scan rate, the electrode radius and the diffusion coefficient.

However, from the Einstein–Smoluchovsky theory of diffusion statistics, the average distance that a free particle with diffusion coefficient D moves in the period of time t is expressed as

$$\Delta = (2Dt)^{1/2} \quad (14)$$

where $t = RT/Fv$ is given as the real experiment time or characteristic time [12]. Thus, $\Delta = (2DRT/Fv)^{1/2}$. When the distance that the particle diffuses from the electrode surface is larger than the thickness of the diffusion layer δ_{ss} ($\delta_{ss} = nFADc_R^*/I_{d(mde)} = \pi r/4$), the particle cannot react at the electrode again (for the sake of simplicity, the diffusion layer is used instead of the reaction layer here), then the ratio of the amount of product that can react inversely at the electrode to

the total amount of product, i.e. the coefficient of retention, is

$$K_s = \delta_{ss}/\Delta = \pi r(Fv/32DRT)^{1/2} \quad (15)$$

It can be seen that the coefficient of retention is proportional to $v^{1/2}$ and r, and is inversely proportional to $D^{1/2}$. The relation is the same as eqn. (1) and in the literature [10]. The coefficient of retention can be calculated theoretically from eqn. (15) with the experimental parameters, and it can also be determined experimentally using eqn. (13). When the radius of the electrode is very large, the diffusion layer thickness is $(\pi Dt)^{1/2}$, and eqn. (15) is not applicable. The coefficient of retention at a macroelectrode or at a very high scan rate is near to unity.

3. Experimental

3.1. Instrumentation

Voltammetric measurements were carried out with a polarecord E506, VA-scanner E612 (Metrohm Switzerland), 3036 type X–Y recorder (Yokogawa Hokushin, Tokyo and Sichun, China), type ATA-1 rotating disk electrode (Jiangsu Electroanalytical Instrument Factory, China), and Jw-0.001°C type thermostat (Chongqing Instrument Factory, China).

A three-electrode configuration was employed. A carbon fiber microdisk electrode ($r = 5$ μm) was used as the working electrode [13]. An SCE with double salt bridge which consisted of saturated KCl solution and 0.1 mol l^{-1} $(C_4H_9)_4NClO_4$ in acetonitrile solution was used as a reference electrode. The experiments were carried out in acetonitrile solution of 1.3×10^{-3} mol l^{-1} ferrocene with 0.1 mol l^{-1} $(C_4H_9)_4NClO_4$ as supporting electrolyte under an inert nitrogen atmosphere.

3.2. Chemicals

Acetonitrile (C.P.) was redistilled as described in the literature [14]. $(C_4H_9)_4NClO_4$ was synthesized from $(C_4H_9)_4NClO_4Br$ (A.R.) and $HClO_4$ (A.R.) as described in the literature [15]. Ferrocene was of analytical reagent grade.

4. Results and discussion

4.1. Voltammetric response at a rotating disk electrode

In Fig. 1, the current increases with increasing rotation speed, and at a fixed scan rate the voltammetric curve tends to a sigmoidal shape. At a low scan rate, there is a linear relation between I and $\omega^{1/2}$ (Fig. 2(A)). At a fixed rotation speed, the current is independent of the scan rate when the scan rate is very low or the rotation speed is very large. However, the curve

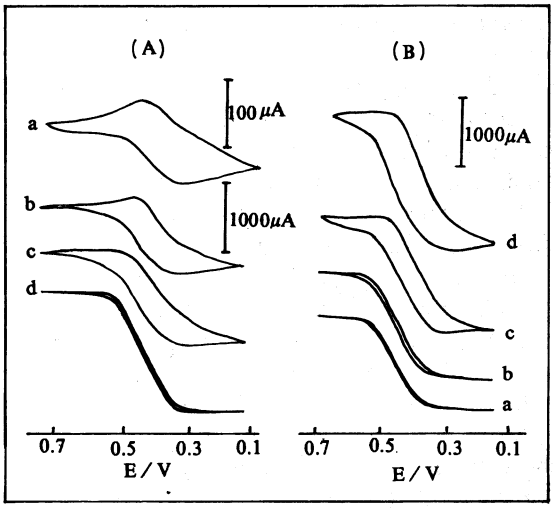

Fig. 1. Cyclic voltammogram of ferrocene at a rotating disk electrode: (A) $v = 200$ mV s^{-1}, $\omega = 0$, 400, 1200 and 2400 rad s^{-1} for curves a–d respectively; (B) $\omega = 1560$ rad s^{-1}, $v = 20$, 100, 400 and 800 mV s^{-1} for curves a–d respectively. Acetonitrile solution of 0.1 mol l^{-1} $(C_4H_9)_4NClO_4$ and 1.3×10^{-3} mol l^{-1} ferrocene.

shows a peak shape at increased scan rate, and the current is proportional to $v^{1/2}$ at a low rotation speed or high scan rate (Fig. 2(B)).

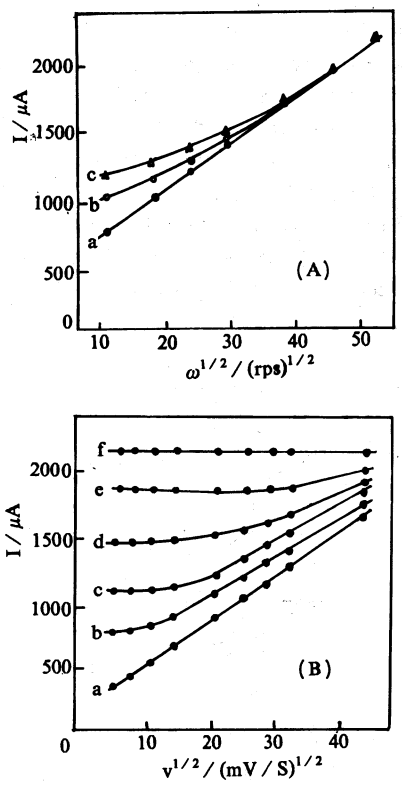

Fig. 2. Relations of (A) I–$\omega^{1/2}$ and (B) I–$v^{1/2}$ at a rotating disk electrode: (A) $v = 100$, 400 and 800 mV s^{-1} for curves a–c respectively; (B) $\omega = 0$, 400, 800, 1560, 2400, 4000 rad s^{-1} for curves a–f respectively. Other conditions the same as for Fig. 1.

4.2. Voltammetric response at a carbon fiber microdisk electrode

In Fig. 3, the sigmoidal curve, with overlapping forward and backward sweep branches, begins to separate with increasing scan rate, and changes gradually into a peak shape. This is similar to the shape at a rotating disk electrode. The separation of the two curves forms the cycle of retention. When $v < 100$ mV s^{-1} the current I is independent of the scan rate, and when $v > 400$ mV s^{-1} I increases with $v^{1/2}$. This is similar to the cases between curves d and e in Fig. 2(B). As is well known, the diffusion coefficient of ferrocene is 2.4×10^{-5} cm^2 s^{-1}, the kinematic viscosity of acetonitrile is 4.37×10^{-3} cm^2 s^{-1} (20 °C), then $\omega = 2259$ rad s^{-1} ($1/2\pi$ s^{-1}) from eqn. (5). This falls in the range 1560–2400 rad s^{-1}.

4.3. Chronoamperometric curves

In Fig. 4, the current quickly reaches a constant value at the microdisk electrode. At the glassy carbon macroelectrode, I decreases with $t^{-1/2}$, and tends to a steady value after very long times (Fig. 4(B)). At the rotating disk electrode, I tends to a constant value more quickly with increasing ω, and increases with $\omega^{1/2}$. From a comparison between Figs. 4(A) and 4(C), it can be estimated that the time to reach a constant current value at the microdisk electrode is identical with that at the rotating disk electrode when the rotation speed is in the range 1560–2400 rad s^{-1}. This means that eqns. (5) and (7) are valid.

As seen in Fig. 4, there is a rise-time in the curves of j–t owing to double-layer capacitance and the inertia of the recorder. Therefore, the origin of the t-axis must be corrected, i.e. point 0′ is approached as the origin of the t-axis (Fig. 4(B)). The limiting steady-state current density at the microdisk electrode for ferrocene measured from Fig. 4(A) (curves 3,4) is 6 mA cm^{-2}, thus the calculated values of current density from eqn. (6) at a glassy carbon electrode are 0.54, 0.38, 0.27 and 0.22 mA cm^{-2} when $t = 0.25$, 0.5, 1.0 and 1.5 s. The results are very close to the experimental values of 0.53, 0.35, 0.25 and 0.20 mA cm^{-2} measured directly from Fig. 4(B) for the same interval time. The theoretical value of j_{ss}/j_{rde} for ferrocene is $47.8/\omega^{1/2}$ obtained from eqn. (7). The slope of j vs. $\omega^{1/2}$ (in Fig. 4(C)) is 0.123 at the rotating disk electrode; thus the experimental value of j_{ss}/j_{rde} is $48.7/\omega^{1/2}$. These results also prove the validity of eqns. (5), (6) and (7).

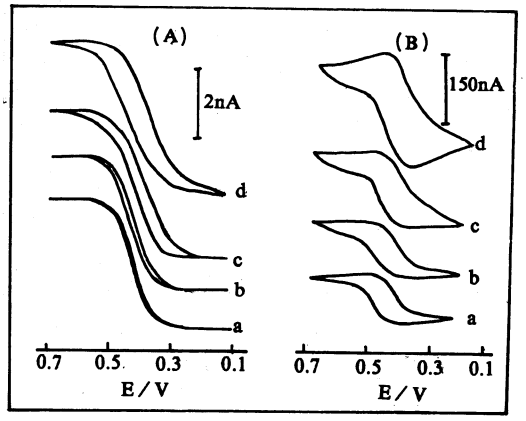

Fig. 3. Cyclic voltammograms at a carbon fiber microdisk electrode: (A) $v = 5$, 100, 400 and 800 mV s^{-1} for curves a–d respectively; (B) $v = 35$, 50, 80 and 100 V s^{-1} for curves a–d respectively. Other conditions the same as for Fig. 1.

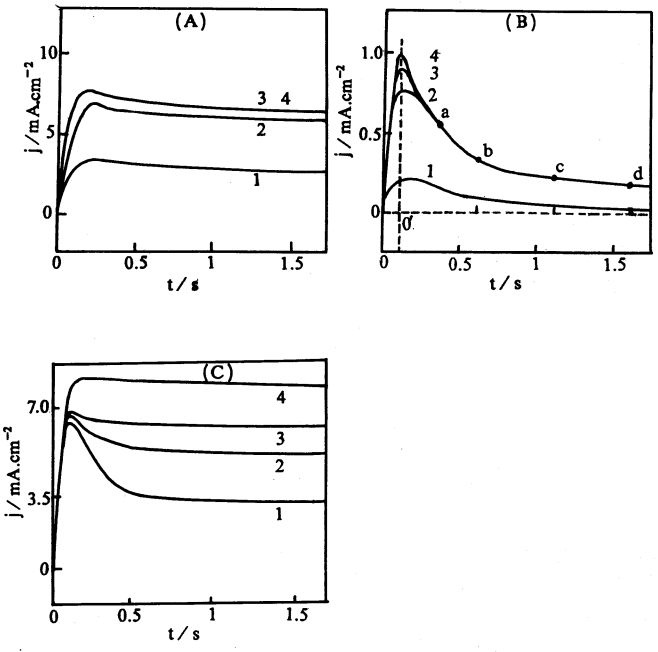

Fig. 4. Chronoamperometric curves at (A) a microelectrode, (B) a glassy carbon macroelectrode, and (C) a rotating disk electrode with potentials of 0.4, 0.5, 0.6 and 0.7 V for curves 1–4 respectively in (A) and (B) and a potential of 0.6 V with $\omega = 400$, 1560, 2400 and 4000 rad s^{-1} for curves 1–4 respectively in (C). Acetonitrile solution of 0.1 mol l^{-1} $N(C_4H_9)_4ClO_4$ and 1.3×10^{-3} mol l^{-1} ferrocene.

4.4. Inverse current at the microdisk electrode

With increasing scan rate, the cyclic voltammogram at the microdisk electrode gradually becomes a cycle. In the course of the backward sweep, the electrode process contains two electrode reactions (oxidation of the reactant and reduction of the product). Thus the total current contains the oxidation current of the reactant, the reduction current of the product and the charging current. It can be seen that the charging current is much smaller than the Faradaic current. Thus the current determined from the voltammogram can be considered as the Faradaic current. From eqns. (8) and (9), the distance between the curves of the

TABLE 1. Reduction current in the backward sweep I_R/nA

E/V	Scan rate/mV s^{-1}										
	5	20	40	60	80	100	200	400	600	800	1000
0.30	0.000	0.013	0.019	0.028	0.042	0.045	0.068	0.087	0.167	0.223	0.334
0.35	0.000	0.031	0.123	0.131	0.185	0.199	0.340	0.537	0.695	0.738	0.958
0.40	0.000	0.117	0.216	0.297	0.376	0.429	0.638	0.961	1.20	1.39	1.66
0.42	0.000	0.173	0.251	0.334	0.405	0.476	0.680	1.00	1.25	1.44	1.69
0.45	0.000	0.105	0.197	0.246	0.329	0.363	0.568	0.808	1.02	1.26	1.40
0.50	0.000	0.016	0.033	0.071	0.108	0.119	0.221	0.380	0.556	0.638	0.750
0.55	0.000	0.003	0.010	0.033	0.048	0.056	0.070	0.118	0.200	0.278	0.408
0.60	0.000	0.000	0.000	0.000	0.000	0.000	0.000	0.010	0.016	0.037	0.089
Oxidation limiting current/mA	4.18	4.18	4.18	4.18	4.18	4.20	4.25	4.37	4.63	4.65	4.69

forward and backward sweeps is the current caused by the reduction (i.e. inverse) reaction of the product, provided that the charging current is neglected. The currents of the inverse reaction for ferrocene at a microdisk electrode at various scan rates are shown in Table 1. With increasing scan rate, the reduction current increases, and all the maximum values occur at the half-wave potential at various scan rates. At the beginning of the backward sweep, c_O^s is the largest, but the reduction rate is the lowest owing to the very positive potential; I_R is very small. As the potential becomes more negative, the reduction rate increases, and I_R increases in spite of the decreasing c_O^s. As the potential becomes more negative than the half-wave potential, although the reaction rate increases, the current is lower than that at the half-wave potential and tends to zero because of diffusion of the product. With increasing scan rate, the time for diffusion reduces, and the current of the inverse reaction increases.

4.5. Coefficient of retention of the product

The formula for calculation of the coefficient of retention K_s is given by eqn. (13). K_s shows the amount of product remaining in the reaction layer on the electrode surface. It can be seen from Table 2 that the maximum of K_s appears at the half-wave potential, and increases with increasing scan rate. This is also due to the reduction current being affected by both the potential and the concentration of product remaining in the reaction layer.

4.6. Data analysis for the coefficient of retention

When the radius of the electrode is very small, the first term in eqn. (1) can be neglected, and I_R/I_O is proportional to $rv^{1/2}$. Thus I_R is proportional to $v^{1/2}$ under the conditions of fixed radius. The same relation of K_s and $v^{1/2}$ is given in eqn. (15). In Fig. 5, the plot of K_s vs. $v^{1/2}$ shows good linearity. All these results can confirm eqns. (1) and (15).

Given $D = 2.4 \times 10^{-5}$ cm^2 s^{-1}, the values of δ_{ss}/Δ for various radii and various scan rates can be obtained from eqn. (15) (shown in Table 3). When the radius is 5 μm, δ_{ss}/Δ is close to the experimental coefficient of retention for ferrocene at the half-wave potential. The experimental slope of K_s vs. $v^{1/2}$ is 0.362 at the half-wave potential, and the slope of δ_{ss}/Δ vs. $v^{1/2}$ is 0.354. At $v = 1000$ mV s^{-1}, $K_s = 0.36$ at the half-wave potential and $\delta_{ss}/\Delta = 0.355$. These results not only verify eqn. (15), but also indicate that K_s at the half-wave potential is the characteristic coefficient of retention.

If the electrode radius or the scan rate is larger, eqn. (15) is no longer applicable owing to the presence

TABLE 2. K_s of the product at a carbon fiber microdisk electrode

E/V	V/mV s^{-1}										
	5	20	40	60	80	100	200	400	600	800	1000
0.30	0.000	0.0031	0.0045	0.0067	0.010	0.011	0.016	0.020	0.036	0.048	0.071
0.35	0.000	0.0074	0.026	0.031	0.044	0.047	0.080	0.12	0.15	0.18	0.20
0.40	0.000	0.028	0.052	0.071	0.090	0.10	0.15	0.22	0.26	0.30	0.35
0.42	0.000	0.042	0.060	0.080	0.097	0.11	0.16	0.23	0.27	0.31	0.36
0.45	0.000	0.025	0.047	0.059	0.079	0.085	0.13	0.18	0.22	0.27	0.30
0.50	0.000	0.0038	0.008	0.017	0.026	0.028	0.052	0.087	0.12	0.14	0.16
0.55	0.000	0.0007	0.0024	0.0079	0.011	0.013	0.016	0.027	0.043	0.060	0.087

TABLE 3. Dependence of δ_{ss}/Δ on the scan rate for various radii

Radius/μm	Scan rate/mV s^{-1}							v/mV s^{-1} for $\delta_{ss}/\Delta = 1$
	20	60	100	200	400	600	1000	
20	0.199	0.347	0.447	0.663	0.895	1.10	1.42	517
10	0.0995	0.173	0.223	0.317	0.248	0.550	0.710	1939
5	0.0497	0.0867	0.112	0.0158	0.224	0.275	0.355	7759
2	0.0199	0.0347	0.0447	0.0633	0.0895	0.110	0.142	49840
1	0.0100	0.0173	0.0223	0.0317	0.0248	0.0550	0.0710	193980
0.5	0.0050	0.0087	0.0112	0.0158	0.0224	0.0275	0.0355	798000
r/μm for $\delta_{ss}/\Delta = 1$	100	58	45	32	22	18	14	

of both linear and non-linear diffusion. The scan rates for various radii and the radii for various scan rates in the case of $\delta_{ss}/\Delta = 1$, in which linear diffusion is predominant for a given radius or scan rate, are also listed in Table 3. The calculations also show that the limiting potential scan rate is 12 V s^{-1} at $r = 4$ μm; this is close to the result in the literature [3] that at $v = 10$ V s^{-1} a peak appeared in the voltammogram. The calculations give a limiting radius of 64 μm at $v = 50$ mV s^{-1} which is also in agreement with the results in the literature [3].

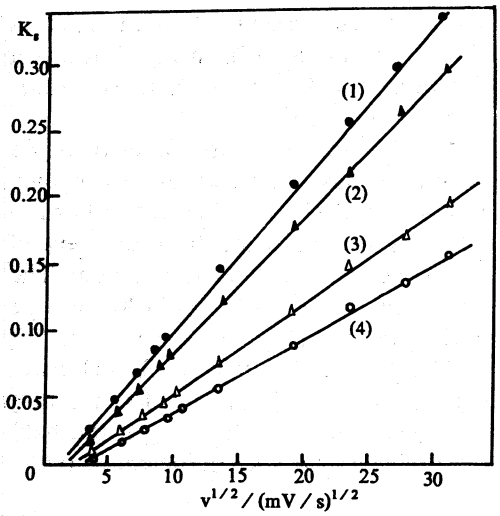

Fig. 5. Dependence of the coefficient of retention on $v^{1/2}$ at a carbon fiber microdisk electrode in acetonitrile solution of 0.1 mol l^{-1} $N(C_4h_9)_4ClO_4$ and 1.3×10^{-3} mol l^{-1} ferrocene at 0.40, 0.45, 0.35 and 0.50 V for curves 1–4 respectively.

Acknowledgment

This project was supported by the National Natural Science Foundation of China.

References

1 R.M. Wightman, Anal. Chem., 53 (1981) 1125A.
2 Huangxian Ju and Hongyuan Chen, Chem. Sensors 10 (1) (1990) 1 (in Chinese).
3 Z. Galus, J.O. Schenk and R.N. Adams, J. Electroanal. Chem., 135 (1982) 1.
4 H. Reller, E. Kirowa-Eisner and E. Gileadi, J. Electroanal. Chem., 138 (1982) 65.
5 A.M. Bond, K.B. Oldham and C.G. Zoski, Anal. Chim. Acta, 216 (1989) 177.
6 A.M. Bond, K.B. Oldham and C.G. Zoski, J. Electroanal. Chem., 245 (1988) 71.
7 J. Cassidy, J. Ghorghchian, F. Sarfarazi, J. Smith and S. Pons, Electrochim. Acta, 31 (1986) 629.
8 Changmin Li, Huaxue Tongbao, (1) (1987) 33 (in Chinese).
9 Sinru Lin and R.A. Osteryoung, Anal. Chem., 60 (1988) 1845.
10 C.G. Zoski, A.M. Bond, C.L. Colyer, J.C. Myland and K.B. Oldham, J. Electroanal. Chem., 263 (1989) 1.
11 K. Aoki, K. Akimto, K. Tokuda, H. Matsuda and J. Osteryoung, J. Electroanal. Chem., 171 (1984) 219.
12 H.A.O. Hill, A. Napthali, I. Psalti and N.J. Walton, Anal. Chem., 16 (1989) 2200.
13 Hongyuan Chen and Huangxian Ju, Chem. Sensors, 8 (4) (1988) 34 (in Chinese).
14 J.F. Coetzee, Anal. Chem., 34 (1962) 1139.
15 I.M. Koltheff and J.F. Coetzee, J. Am. Chem. Soc., 79 (1959) 870.